SMAR 2019 – Fifth Conference on Smart Monitoring,
Assessment and Rehabilitation of Civil Structures

SMAR 2019

Performance of Continuous Concrete Beams with Reinforced FRP Bars and Sheets

Salvio ARAGAO ALMEIDA JUNIOR [1], Azadeh PARVIN [1]

[1] The University of Toledo, Toledo, USA

Contact e-mail: azadeh.parvin@utoledo.edu

ABSTRACT: The growing use of fiber-reinforced polymer (FRP) composites has led to the development of new fibers, such as basalt sheets and bars. While basalt has an excellent tensile strength, its external use as sheets can be hindered by debonding. One way to overcome this issue is to replace the normal strength concrete (NSC) with ultra-high-performance fiber-reinforced concrete (UHPFRC), which has superior bond with FRP. However, this material is more expensive than NSC. In the present numerical study partial use of UHPFRC was proposed to investigate the cases of (a) a continuous beam reinforced with carbon, glass, and basalt bars and (b) a steel-reinforced beam strengthened with same fiber types in the form of sheets. A cost analysis was performed to assess the feasibility of each case. The results revealed significant increase in the beam's load capacity and successful prevention of debonding at a cost 81% lower than the full use of UHPFRC.

Keywords: UHPFRC, Basalt fibers, FRP-concrete bond, FRP bars, FRP sheets, Strengthening.

1 INTRODUCTION

Recent advancements in concrete technology have led to the development of ultra high-performance fiber-reinforced concrete (UHPFRC). This material has superior properties as compared to regular concrete, such as lower permeability and a stronger bond with FRP bars and sheets (Brühwiler 2016; Ueda and Dai 2005). FRP external bonding provides an excellent retrofit option given that not only it increases the structural strength, but also it resists corrosion, thus providing structural durability. However, a major drawback of this type of strengthening is the premature debonding of the sheets, as reported by Khalifa (2016). The use of UHPFRC in the tension zone of the beam or as an external layer can provide a solution to this problem.

Full replacement of the normal-strength concrete (NSC) by UHPFRC in a beam is known to increase the bond between concrete and FRP reinforcement bars, as well as the flexural strength of the beam (Almeida Jr. and Parvin 2019). On the other hand, such applications can be costly. Therefore, partial replacement of the NSC with UHPFRC may be a more feasible alternative.

UHPFRC has been used as an external layer in Switzerland to create a protective surface and increase the durability of the concrete (Brühwiler 2016). Recent investigations of alternative manufacturing of UHPFRC, e.g. Amanjean and Vidal (2014), indicate that its cost can be brought down, making UHPFRC more viable for daily construction practices in the future.

In the present numerical study, the effects of partial replacement of NSC with UHPFRC in continuous beams reinforced with FRP bars and sheets are investigated. Finite element analysis (FEA) models were developed and validated with experimental data from Ashour and Habeeb (2008) and FEA and test results were in good agreement (Almeida Jr. and Parvin 2019). Two of the validated models were modified to investigate the effects of full and partial UHPFRC

replacement. Carbon, glass, and basalt bars were used as the main reinforcement in one case and as externally applied sheets for the strengthening of a steel reinforced concrete beam in another. A cost analysis was performed to investigate the feasibility of the proposed alternative.

2 FINITE ELEMENT ANALYSIS MODELING OF THE BEAMS

The details of FEA beam models are presented in Figure 1. Since the beams were symmetric, only their right half was modeled, and symmetry boundary conditions were applied at the left end. The results of two beam models, previously validated with experimental study by Ashour and Habeeb (2008) and presented in Almeida Jr. and Parvin (2019), were compared to the present parametric study results. The first beam was cast with 28 MPa concrete and reinforced with two CFRP bars at the top and bottom and CFRP stirrups with 140 mm spacing (Figure 1a). It was used to study the effects of partial and full replacement of the concrete with UHPFRC using carbon, glass, and basalt fibers as the main reinforcement. The second beam had a concrete compressive strength of 26.8 MPa and was reinforced with four steel bars at top and bottom and steel stirrups were spaced at 140 mm (Figure 1b). This model was retrofitted with carbon, glass, and basalt FRP sheets at the positive moment region and NSM bars at the negative moment region and used to study the effects of adding a thin layer of UHPFRC at the bottom of the beam to strengthen the concrete-FRP sheet bond. The reinforcement material properties are summarized in Table 1.

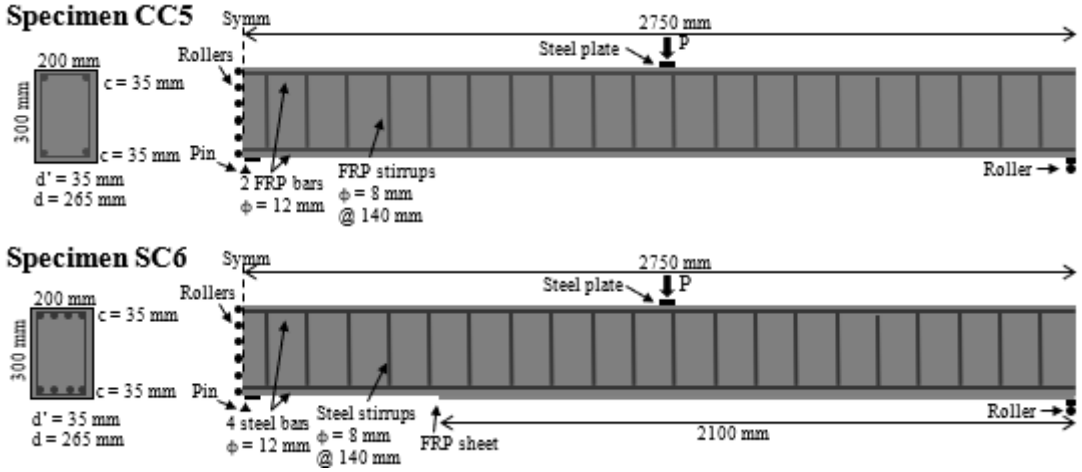

Figure 1. Geometry boundary conditions and reinforcement details of the beam models.

Table 1. Material properties of the reinforcement bars and sheets

Material	**E (GPa)**	**f_y (MPa)**	**f_u (MPa)**	**ε_u -**	**ε_{fu} -**
Steel stirrups	206.8	525.5	611.6	0.15	-
Longitudinal steel bars	200	510.8	594.4	0.15	-
CFRP bar	200	-	1061	-	0.0053
GFRP bar	60	-	1000	-	0.0167
BFRP bar	59.5	-	1567	-	0.0263
CFRP sheet	230	-	3820	-	0.0166
GFRP sheet	73	-	780	-	0.0107
BFRP sheet	81.5	-	2145	-	0.0263

The concrete constitutive models are shown in Figures 2 (a and b). The formulation proposed by Popovics (1973) was used to model the compressive response of concrete until its peak strength was reached. After that, the stress was decreased linearly up to a residual value equal to 20% of its peak strength. The concrete tensile strength was described as a linear-elastic branch up to cracking followed by a tension stiffening formulation to define the post-crack response.

A typical elastic-plastic model with nonlinear strain hardening was used to model the steel bars. The FRP bars and sheets had a linear-elastic behavior with the rupture at ultimate strain (ε_{fu}). The bond between the concrete and the FRP composites was modeled with a linear increasing branch up to the peak strength, then a linear decreasing branch and a residual strength afterwards (Figure 2c), with the key parameters calculated as per Gravina and Smith (2008), Elgabbas et al. (2015), and Yan and Lin (2016).

The bond strength between CFRP and GFRP bars and the UHPFRC was obtained from Firas (2011) and Yoo (2015), respectively. No experiment was found measuring the bond between BFRP bars and UHPFRC. However, Ueda and Dai (2005) reported a successful model that predicts the bond between FRP and the concrete, which was proportional to $f'c^{1/2}$. Their analytical model was used in the present study to calculate the bond between BFRP bars and UHPFRC.

The two-dimensional finite element software VecTor2 was used to create and analyze the beams. The concrete was modeled as a continuum with 2-D rectangular elements containing smeared transversal reinforcement. The steel and FRP longitudinal bars and sheets were modeled as 1-D truss elements. Link elements were used to define the bond between concrete and reinforcement bars or external sheets.

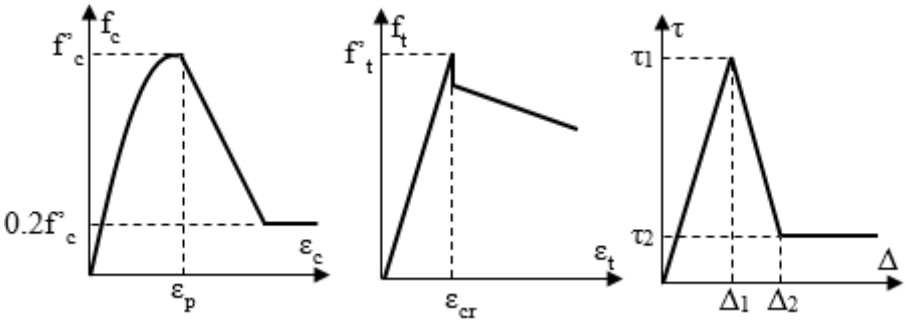

(a) (b) (c)

Figure 2. Concrete (a) compressive; and (b) tensile stress-strain curves; and (c) bond stress-slip curve.

3 DISCUSSION OF RESULTS

In the following sections, comparison of (a) partial UHPFRC with full UHPFRC and NSC beams reinforced with various FRP bars, and (b) NSC and partial UHPFRC steel reinforced beams externally strengthened with various FRP NSM bars and sheets are made. Finally, effect of bond strength on the beam's load capacity is also discussed.

3.1 Comparison of partial/full UHPFRC and NSC beams reinforced with various FRP bars

The previously analyzed beam models fully cast with NSC (f'c = 28 MPa) and UHPFRC (f'c = 170 MPa) found in Almeida Jr. and Parvin (2019) were also simulated with partial use of UHPFRC above the bottom layer of FRP bars in the tension zone. In this scenario, a 50 mm-thick

layer of UHPFRC was applied at the positive moment regions to surround the reinforcing bars. The main objective was to provide a similar high bond between concrete and tensile bars as the beam with full UHPFRC. This approach would result in minimizing the cost associated with UHPFRC material while improving durability by using less permeable concrete in the most exposed zone of the beam.

The load versus displacement responses of the beams are compared in Figure 3. The use of UHPFRC as a full replacement for NSC slightly increased the load capacity of the beam. However, as compared to NSC, the beam's cost greatly increased (Figure 4a). The partial use of UHPFRC was 81% less expensive than the full replacement and allows taking advantage of the improved concrete-FRP bond, which can be significantly stronger as compared to NSC (Figure 4b). In addition, as compared to the beam with full UHPFRC, a higher displacement capacity was observed in the beam with partial UHPFRC, which gives more warning before failure. Therefore, the use of a thin layer of UHPFRC replacing NSC at the positive moment regions of the beam is recommended if an increase in bond strength is desired.

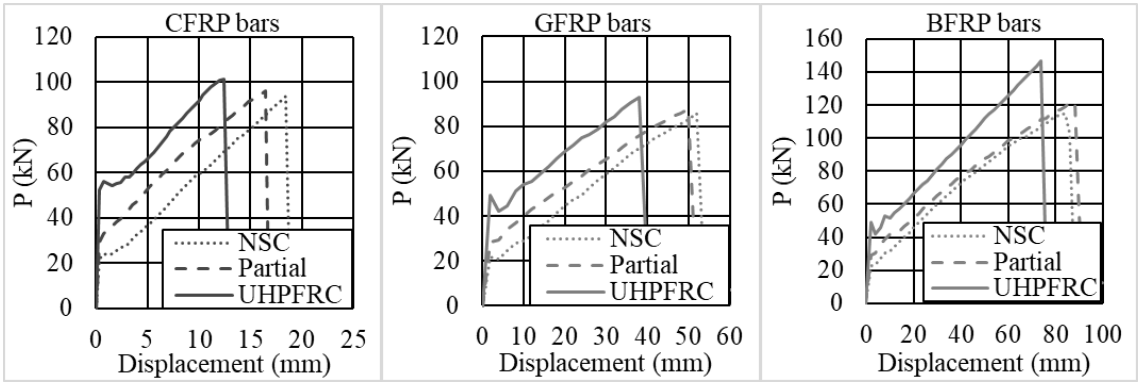

Figure 3. Load versus displacement curves of continuous beam models.

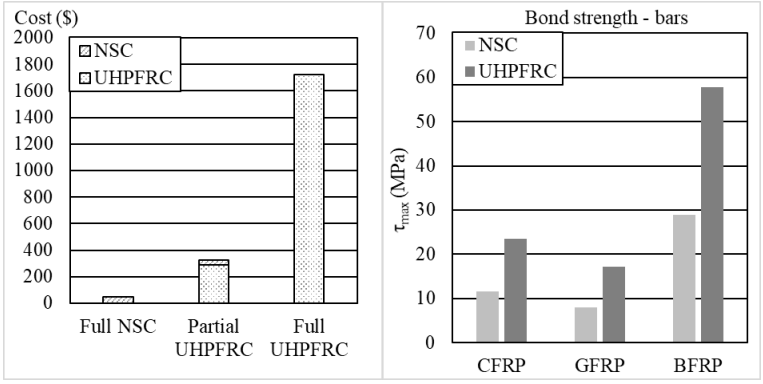

(a) (b)

Figure 4. Comparison of NSC and UHPFRC beams in terms of (a) cost; (b) bond strength.

3.2 Comparison of NSC and partial UHPFRC steel reinforced beams externally strengthened with various FRP NSM bars and sheets

Many existing steel reinforced concrete beams are in need of retrofit. In this section, the FEA model of steel-reinforced control beam by Almeida Jr. and Parvin (2019) is used to perform additional parametric study for external strengthening. In the first stage of the study, external CFRP, GFRP, and BFRP sheets were added in the positive moment zone of the continuous beam with NSC. In the second stage, the NSC in contact with the sheets was replaced by a 50 mm layer of UHPFRC. In the final stage of the study, NSM FRP bars were added in the negative moment zone. The NSM bars' material types were selected to be the same as the sheets for each beam case study. The objectives were to investigate the effects of adding external sheets and NSM bars on the load capacity and to enhance the concrete-FRP bond while maintaining the cost at minimum. The FRP reinforcement bars were extended beyond the positive and negative moment zones by their development length, calculated according to ACI 440 (see Table 2). Table 3 shows the properties of the sheets and their bond with the NSC (τ) and UHPFRC (τ') concrete layers, obtained from Ali-Ahmad et al. (2006), Jia et al. (2005), and Shi et al. (2013). The selected sheets were 180 mm wide and 0.167 mm thick in all models. It was assumed that the concrete type did not affect the slip of the bond stress-slip curve.

Table 2. FRP development length

Fiber	L_{NSC} (mm)	L_{UHPFRC} (mm)
CFRP bar	461	461
GFRP bar	435	435
BFRP bar	681	681
CFRP sheet	87	54
GFRP sheet	49	30
BFRP sheet	52	32

Table 3. FRP sheets properties

Fiber material	E (GPa)	f_u (MPa)	τ_1 (MPa)	Δ_1 (mm)	τ_2 (MPa)	Δ_2 (mm)	τ'_1 (MPa)	Δ'_1 (mm)	τ'_2 (MPa)	Δ'_2 (mm)
Carbon	230	3820	3.9	0.05	0.05	0.37	9.9	0.05	0.10	0.37
Glass	72.4	1517	2.6	0.05	0.00	0.25	6.7	0.05	0.00	0.25
Basalt	81.5	2145	6.4	0.06	0.73	0.32	16.2	0.06	1.85	0.32

The load versus displacement curves of all beam models are presented in Figure 5. Application of FRP sheets to the NSC control beam resulted in a noticeable increase in the load capacity. With the use of BFRP sheet, a slight reduction in displacement capacity was observed. This happened because while the control model reached a plateau after yielding of the tensile steel reinforcement, the load in the strengthened beams continued to increase due to extra capacity provided by the FRP sheets. Consequently, a concentration of stresses formed around the left pin support causing local crushing of the concrete shortly after the load surpassed the capacity of the control beam (Figure 6a).

The use of a thin layer of UHPFRC at the bottom of the beams significantly improved their load and displacement capacities when CFRP and BFRP sheets were used. The main reason for that was that the stronger concrete around the support was not susceptible to crushing, therefore

shifting the failure mode to the rupture of the sheets. The load gain was more pronounced when CFRP sheets were used due to their higher tensile strength (see Table 3).

In all cases, severe cracking was observed at midspan and on the left end support. In the beam model with partial UHPFRC, a major opening above the sheet occurred at failure [Figure 6 (b)]. Some cracking above the UHPFRC layer was also observed to propagate from the left end in this case. Furthermore, partial use of UHPFRC significantly enhanced the concrete-FRP bond (Figure 7), however, this effect altered the load versus displacement response slightly, since debonding of the sheets was not an issue in the retrofit case studies. Lastly, the addition of NSM further increased the load capacity, but also led to a slight reduction in the displacement at failure. Both phenomena are likely due to the redistribution of stresses caused by the NSM.

While UHPFRC is beneficial in improving the concrete-FRP bond (Figure 7), similar to the previous case study, its use should be limited to a thin layer in order to avoid an excessive cost increase. However, with the advancement in technology, the UHPFRC cost could be brought down. Therefore, partial and complete uses of UHPFRC as an alternative to NSC are likely to become a more viable option in the near future.

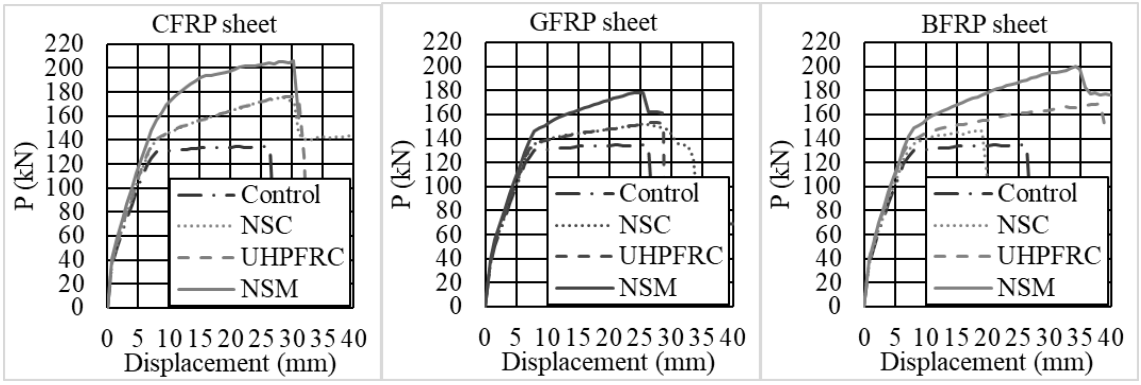

Figure 5. Load versus displacement curves of SC6 beam reinforced with CFRP, GFRP, and BFRP sheets.

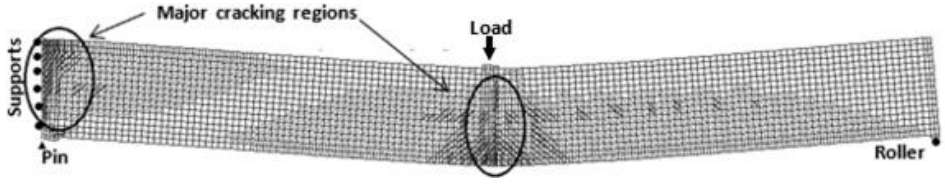

(a) NSC-BFRP

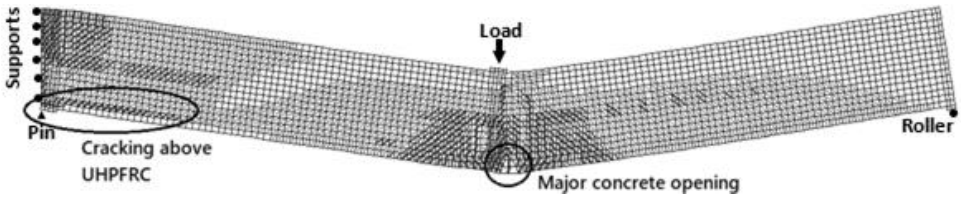

(b) UHPFRC-BFRP

Figure 6. Failure cracking pattern of retrofitted beams (a) NSC-BFRP sheets; (b) UHPFRC-BFRP sheets.

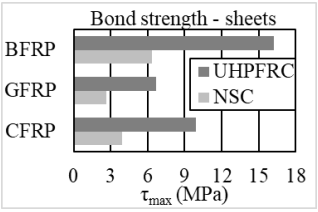

Figure 7. FRP sheet-concrete bond for all the fibers and concrete types.

3.3 Effect of bond strength on the beam's load capacity

In this section the debonding phenomenon was investigated by changing the bond strength in the partial UHPFRC beam reinforced with GFRP bars and in the NSC steel reinforced beam retrofitted with GFRP sheets. When the bond strength between concrete and GFRP tensile reinforcement bar was increased (Figure 8), there was virtually no effect prior to reaching concrete cracking load (phase I). After that, the load capacity increased almost linearly (phase II) until the debonding strength surpassed the fiber strength (phase III), at which point debonding no longer occurred, and therefore increasing the bond had no effect. The transitions between phase I and II, and phase II and III occurred approximately at 1 MPa and 3.5 MPa bond strength, respectively. For the second beam with GFRP sheet (Figure 8), the load capacity of the beam increased from the beginning (phase I) due to the presence of internal steel combined with GFRP sheet reinforcement. Beyond certain bond strength, rupture of the sheet started to govern the failure and increase in bond strength was irrelevant (phase II). The transition between phases I and II occurred at a bond strength of approximately 3 MPa.

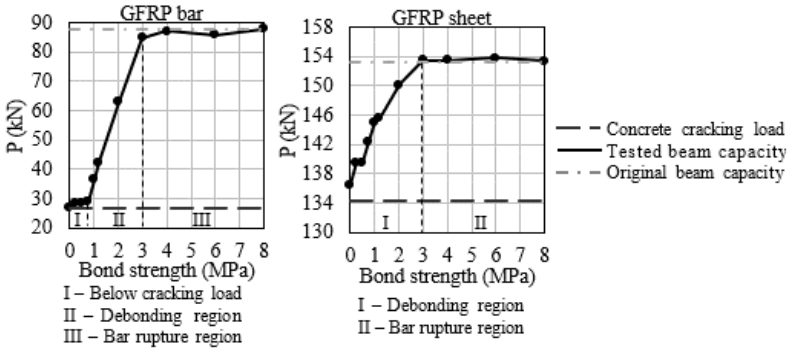

Figure 8. Effect of bond strength on the load capacity of the beams with GFRP bar and FRP sheet.

4 CONCLUSIONS

In the present study, potential advantages and disadvantages of partial replacement of normal strength concrete (NSC) by ultra-high performance fiber-reinforced concrete (UHPFRC) in continuous beams reinforced with fiber-reinforced polymer (FRP) bars and external sheets were numerically investigated. The finite element analysis beam models, previously validated with experimental results, were used to analyze several cases, including the use of NSC, UHPFRC, near-surface mounting (NSM), and UHPFRC in FRP-reinforced beams, and strengthening of steel-reinforced beams with FRP sheets and NSM FRP bars. Carbon, glass, and basalt fibers were selected as reinforcement. A cost analysis comparing NSC and UHPFRC beams was also performed. The main conclusions drawn from this study are as follows:

- Full replacement of NSC by UHPFRC was an excessively expensive option.
- Partial replacement of NSC by UHPFRC was nearly five times (or 81%) cheaper than full replacement. In the meantime, the bond was improved equally. Therefore, the use of a thin layer (e.g. 50 mm) of UHPFRC is recommended in cases where this solution is desired.
- The addition of externally bonded FRP sheets to NSC steel-reinforced beam model significantly increased its load capacity. However, it led to local crushing of the concrete around the middle support. The use of a thin layer of UHPFRC prevented this failure, allowing the beam to develop extra displacement and support a higher load.
- The addition of NSM bars in the negative moment region of the steel reinforced beam models containing FRP sheets and a thin layer of UHPFRC resulted in even higher load capacity without significantly changing the displacement capacity of the beam.
- Below a critical bond strength, debonding of the FRP bars and sheets was the governing mode of failure. When debonding occurred, the load capacity versus bond strength relationship was almost linear. For the two cases studied here, the critical bond strength was 3 MPa.

5 REFERENCES

A. Almeida Jr., S., and A. Parvin, 2019, Behavior of continuous concrete beams reinforced with basalt bars. *Interdependence between Structural Engineering and Construction Management*, STR-66: 6 pp.

Ali-Ahmad, M., K. Subramaniam, and M. Ghosn, 2006, Experimental investigation and fracture analysis of debonding between concrete and FRP sheets. *Journal of Engineering Mechanics*, 132(9): 914-923.

Amanjean, E. N., and T. Vidal, 2014, Low cost ultra-high performance fiber reinforced concrete (UHPFRC) with flash metakaolin. *Key Engineering Materials*, 629-320: 55-63.

Ashour, A. F., and M. N. Habeeb, 2008, Continuous concrete beams reinforced with CFRP bars. *Proceedings of the Institution of Civil Engineers–Structures & Buildings*, 161(6): 349-357.

Brühwiler, E., 2016, "Structural UHPFRC": welcome to the post-concrete era! *First International Interactive Symposium on UHPC*, 16 pp.

Elgabbas, F., E. A. Ahmed, and B. Benmokrane, 2015, Physical and mechanical characteristics of new basalt-FRP bars for reinforcing concrete structures. *Construction and Building Materials*, Elsevier, 95: 623-635.

Firas, S. A., F. Gilles, and L. R. Robert, 2011, Bond between carbon fibre-reinforced polymer (CFRP) bars and ultra-high performance fibre reinforced concrete (UHPFRC): experimental study. *Construction and Building Materials*, 25(2): 479-485.

Gravina, R. J., and S. T. Smith, 2008, Flexural behaviour of indeterminate concrete beams reinforced with FRP bars. *Engineering Structures*, Elsevier, 30(9): 2370-2380.

Jia, J., T. E. Boothby, C. E. Bakis, and T. L. Brown, 2005, Durability evaluation of glass fiber reinforced-polymer-concrete bonded interfaces. *Journal of Composites for Construction*, 9(4): 348-359.

Khalifa, A. M., 2016, Flexural performance of RC beams strengthened with near surface mounted CFRP Strips. *Alexandria Engineering Journal*, 55(2): 1497-1505.

Popovics, S., 1973, A numerical approach to the complete stress-strain curve of concrete. *Cement and Concrete Research*, 3(5): 583-599.

Shi, J., H. Zhu, Z. Wu, M., R. Seracino, and G. Wu, 2013, Bond behavior between basalt fiber-reinforced polymer sheet and concrete substrate under the coupled effects of freeze-thaw cycling and sustained load. *Journal of Composites for Construction*, 17(4): 530-542.

Ueda, T., and J. Dai, 2005, Interface bond between FRP sheets and concrete substrates – properties, numerical modeling, and roles in member behaviors. *Progress in Structural Engineering and Materials*, 7(1): 27-43.

Yan, F., and Z. Lin, 2016, bond behavior of GFRP bar-concrete interface: damage evolution assessment and FE simulation implementations. *Composite Structures*, 155: 63-76.

Yoo, D.-Y., K.-Y. Kwon, J.-J. Park, and Y.-S. Yoon, 2015, Local bond-slip response of GFRP rebar in ultra-high-performance fiber-reinforced concrete. *Composite Structures*, 120: 53-64.